

BoolGebra: Attributed Graph-learning for Boolean Algebraic Manipulation

Yingjie Li¹, Anthony Agnesina², Yanqing Zhang³, Haoxing Ren², Cunxi Yu¹

¹University of Maryland, College Park, College Park, MD, USA

²NVIDIA, Austin, TX, USA

³NVIDIA, Santa Clara, CA, USA

{yingjiel, cunxiyu}@umd.edu, {aagnesina, yanqingz, haoxingr}@nvidia.com

Abstract—Boolean algebraic manipulation is at the core of logic synthesis in Electronic Design Automation (EDA) design flow. Existing methods struggle to fully exploit optimization opportunities, and often suffer from an explosive search space and limited scalability efficiency. This work presents BoolGebra, a novel attributed graph-learning approach for Boolean algebraic manipulation that aims to improve fundamental logic synthesis. BoolGebra incorporates Graph Neural Networks (GNNs) and takes initial feature embeddings from both structural and functional information as inputs. A fully connected neural network is employed as the predictor for direct optimization result predictions, significantly reducing the search space and efficiently locating the optimization space. The experiments involve training the BoolGebra model w.r.t design-specific and cross-design inferences using the trained model, where BoolGebra demonstrates generalizability for cross-design inference and its potential to scale from small, simple training datasets to large, complex inference datasets. Finally, BoolGebra is integrated with existing synthesis tool ABC to perform end-to-end logic minimization evaluation w.r.t SOTA baselines.

I. INTRODUCTION

Logic optimization is an essential stage in the design automation flow for digital systems as the performance of the system at logic level can have significant impacts on the final chip area, timing closure, and the power efficiency of the system [1]–[8]. Logic optimization is a technology-independent circuit optimization at the logic level, aiming to minimize the logic operations and logic level in the circuit while maintaining the original functionality of the circuit. The key methodologies of modern logic optimization techniques are conducted on multi-level technology-independent representations such as And-Inverter-Graphs (AIGs) [9]–[12] and Majority-Inverter-Graphs (MIGs) [4], [13] of the digital logic, and XOR-rich representations for emerging technologies such as XOR-And-Graphs [14] and XOR-Majority-Graphs [15]. Existing state-of-the-art (SOTA) Directed-Acyclic-Graphs (DAGs) aware Boolean optimization algorithms, such as structural rewriting [9], [16], [17], resubstitution [18], and refactoring [9] in ABC [5], are conducted on the AIG data structure of the design following a domain-specific design concept, i.e., existing algorithms are implemented in a stand-alone fashion with single optimization operation in the single DAG-aware traversal.

However, modern digital designs with increasing complexity encompassing millions of logic gates, engender an expansive exploration space. These designs pose substantial challenges to finding optimal solutions using SOTA standalone optimizations incorporated within extant logic synthesis tools. Two major

complications emerge from such an approach. **Firstly**, a significant amount of potential optimizations are overlooked as the process contemplates only a single optimization operation during the traversal of the AIGs. This lack of holistic consideration could trap the optimization within suboptimal local minima. To illustrate, let us consider node j in Figure 1, which is eligible for refactor operation. However, due to the solitary nature of the current optimization method, opportunities for rewrite optimization are disregarded. **Secondly**, the incorporation of multiple optimization techniques within a single AIG optimization exponentially enlarges the search space. In existing SOTA optimization, the optimization space is $O(N)$ for a design containing N AIG nodes. However, when integrating multiple optimization techniques, such as rewriting, resubstitution, and refactoring within a single traversal, the optimization space escalates to $O(3^N)$. This increase in complexity can pose a significant challenge in searching optimal solutions.

Our work proposes new solutions to AIG optimizations targeting the aforementioned two challenges. First, in existing logic optimizations on AIG, the operation is checked transformability and applied to the AIG node sequentially following the topological order, i.e., the optimization for each node is independent from each other, which provides the opportunity to explore different optimizations for nodes in the single AIG traversal. Thus, BoolGebra aims to discover novel manipulation over Boolean networks by integrating rewriting, resubstitution, and refactoring in single AIG traversal.

Second, to deal with the exponentially increased search space with multiple optimizations, we see the potential for employing machine learning (ML) for electronic design automation (EDA) tasks [19]–[26], as an aid to conventional design solutions. The circuit netlists or Boolean networks are represented as graphs, thus Graph Neural Networks (GNNs) are our natural choice for the logic optimization tasks based on AIGs. Specifically, to provide fast yet accurate optimization guidance for logic optimizations, we propose a graph-learning based neural network, which takes the design AIG as input and produces the optimized AIG result directly. Based on the fast-acquired inference result, the search space is thus shrunk, which aids the logic optimization to locate the optimized solution efficiently. Once the model is well trained, it shows its generalization capability from small, simple to large, complex designs.

The main contributions are summarized as follows:

- We develop a GNN-based predictor with function-aware embedding method for fast estimation of logic optimization performance w.r.t the AIG structure and per node algebraic manipulation assignment.
- Exploit the capabilities of the GNN-based predictor, i.e., BoolGebra, a tool designed for rapid sampling and design space exploration. BoolGebra aims to locate unseen orchestrated Boolean manipulation solutions.
- We evaluate BoolGebra in a variety of optimization scenarios, encompassing both design-specific and cross-design optimization. Through these evaluations, BoolGebra demonstrates robust generalizability across multiple design environments.
- BoolGebra is integrated with the ABC synthesis framework [5], facilitating comprehensive end-to-end AIG reduction evaluation w.r.t ABC SOTAs.

II. PRELIMINARY

A. Boolean Networks and AIGs

A Boolean Network is a directed acyclic graph (DAG) denoted as $G = (V, E)$ with nodes V representing logic gates (Boolean functions) and edges E representing the connections between gates. The input of a node is called its *fanin*, and the output of the node is called its *fanout*. The node $v \in V$ without incoming edges, i.e., no *fanins*, is the *primary input* (PI) to the graph, and the nodes without outgoing edges, i.e., no *fanout*, are *primary outputs* (PO) to the graph. The nodes with incoming edges implement Boolean functions.

And-Inverter Graph (AIG) is one of the typical types of DAGs used for logic manipulation, where the nodes in AIGs are all two-inputs AND gates, and the edges represent whether the inverters are implemented. An arbitrary Boolean Network can be transformed into an AIG by factoring the SOPs of the nodes, and the AND gates and OR gates in SOPs are converted to two-inputs AND gates and inverters with DeMorgan's rule. There are two primary metrics for evaluation of an AIG, i.e., *size*, which is the number of nodes (AND gates) in the graph, and *depth*, which is the number of nodes on the longest path from PI to PO (the largest level) in the graph.

A *cut* C of node v includes a set of nodes of the network. The nodes included in the *cut* of node v are called *leaves*, such that each path from a PI to node v passes through at least one leaf. The node v is called the *root* of the *cut* C . The cut size is the number of its leaves and the node itself. A cut is K -feasible if the number of nodes in the cut does not exceed K . The optimization of Boolean networks can be conducted with the AIGs efficiently [8], [27], [28]. The AIG-based optimization process in the single traversal of the graph usually involves two steps: (1) *transformability check* – check the transformability w.r.t the optimization operation for the current node; (2) *graph updates* (`Dec_GraphUpdateNetwork` in ABC [5]) – apply the applicable optimization operation at the node to realize the transformation and update the graph for the next unseen node.

B. DAG-Aware Logic Synthesis

DAG-aware logic synthesis approaches leverage Boolean algebra at direct-acyclic-graph (DAG) representations to reduce

the logic complexity and size, while preserving the original functionality of the circuit, aiming to the enhanced performance of area, delay, power, etc., in the final digital systems. This process involves a variety of optimization techniques and algorithms, e.g., node rewriting, structural hashing, and refactoring. In this work, we are particularly interested in exploring DAG-aware logic synthesis on AIGs representations.

Rewriting, noted as r_w , is a fast greedy algorithm for optimizing the graph size. It iteratively selects the AIG subgraph with the current node as the root node and replaces the selected subgraph with the same functional pre-computed subgraph with a smaller size to realize the graph size reduction. Specifically, it finds the 4-feasible cuts as subgraphs for the node while preserves the number of logic levels [9]. For example, Figure 1b shows the optimization of the original graph in Figure 1a with r_w . The algorithm visits each node in the topological order and checks the transformability of its cut w.r.t r_w . It will skip the node and visit the next one if not applicable. In Figure 1b, the node j is skipped for r_w , and node $k = efr$ is optimized with r_w , resulting in the node reduction of 2 for the AIG optimization.

Refactoring, noted as r_f , is a variation of the AIG rewriting using a heuristic algorithm [18] to produce a large cut for each AIG node. Refactoring optimizes AIGs by replacing the current AIG structure with a factored form of the cut function. It can also optimize the AIGs with the graph depth. For example, Figure 1c shows the optimization of the original AIG with r_f . The node $j = h(\bar{h} + k)$ is optimized with r_f based on DeMorgan's rule, where $j = hk$, and similarly for the node g . As a result, the optimized graph with r_f has a graph size of 17 with 3 nodes reduction and 2 depth reduction.

Resubstitution, noted as r_s , optimizes the AIG by replacing the function of the node with the other existing nodes (`divisors`) already present in the graph, which is expected to remove the redundant node in expressing the function of the current node. For example, in Figure 1a, the node $g = a\bar{p}$, $p = \bar{b}\bar{c}\bar{d}$, $n = (b + c)a$, $m = ad$, i.e., $g = m + n = \bar{m} \cdot \bar{n}$, which can be resubstituted with node $i = \bar{m} \cdot \bar{n}$, and node p is removed from the graph. As a result, with r_s , the original AIG is optimized in graph size by 1 node reduction.

C. Graph Neural Networks in EDA

Graph learning has emerged as a powerful method for understanding complex relationships in various domains, including social networks, biological systems, and natural language processing. In the context of hardware design, graph learning can be employed to model and analyze the intricate connections among design components, such as gates, wires, and registers, to optimize design performance and effectively analyze design characteristics. For example, dataflow graphs, circuit netlist, and Boolean networks (BNs) can be easily represented as graphs, making graph neural networks (GNNs) a natural fit for classifying sub-circuit functionality from gate-level netlists [19], analyzing the impacts of circuit rewriting [20], predicting arithmetic block boundaries [21], [29], improving the fidelity of early-stage design exploration [30]–[34], hardware security [35], [36], technology mapping [37], [38], etc. However, we

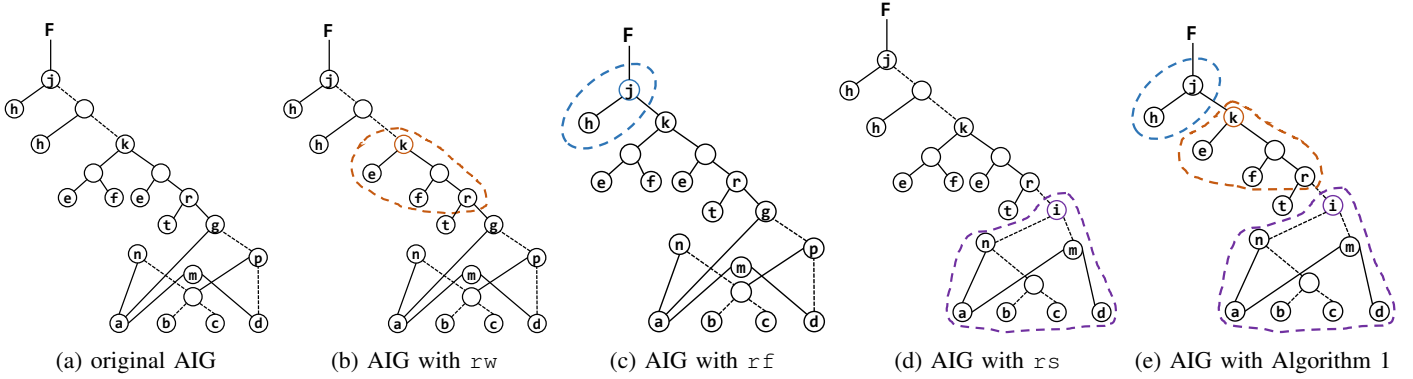


Fig. 1: The optimized graph produced by stand-alone optimization operations and orchestration operation: (a) original AIG, graph size is 21; (b) optimized AIG with stand-alone rw , graph size is 19; (c) optimized AIG with stand-alone rf , graph size is 19; (d) optimized AIG with stand-alone rs , graph size is 20; (e) optimized AIG with proposed Algorithm 1, graph size is 16.

believe there does not exist works in discovering novel Boolean manipulation techniques in fundamental logic synthesis.

decisions for each node in the AIG, including rw , rs , and rf . Each random sample represents a potential Boolean synthesis solution, resulting in an updated AIG. Note that these samples adhere to the principles of Boolean algebra, ensuring the functional equivalence of all generated graphs.

Figure 2 illustrates the results obtained from randomly sampling 6,000 solutions for four different designs (b11, b12, c2670, and c5135) sourced from well-established ITC/ISCAS99 and ISCAS85 benchmarks. Our analysis reveals two key findings. Firstly, the choice of manipulation decisions for the Boolean network graphs significantly impacts the final quality-of-results in logic minimization. Secondly, the distribution of quality-of-results within the randomly sampled design space approximately follows a Gaussian distribution. Consequently, employing a random sampling method for the purpose of logic minimization, specifically in identifying solutions that offer the minimum AIG size, proves to be challenging or infeasible. This study affirms the presence of optimization opportunities and challenges, thereby motivating our work in leveraging graph learning techniques to identify superior Boolean manipulation methods. In Section III, we will further discuss Guided sampling that optimizes our training performance.

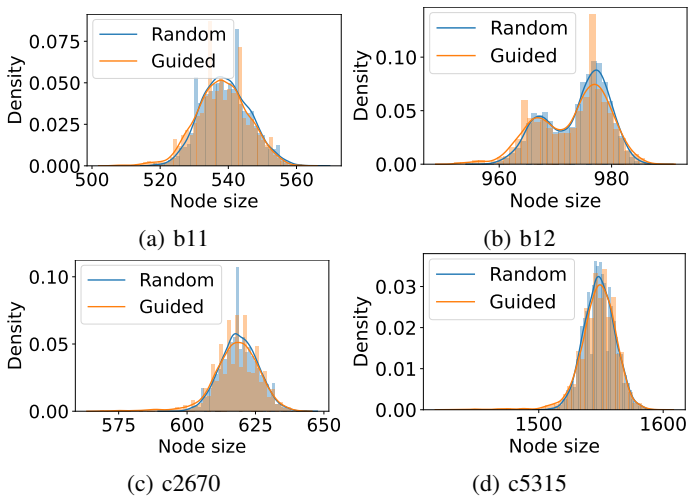


Fig. 2: The optimization quality distribution with 6000 samples of purely random sampling and priority guided sampling.

III. APPROACH

In this section, we first provide the studies on the optimization opportunities in the single traversal of AIG for the orchestration optimization (Section III-A). Then we introduce the method with orchestrating multiple optimizations with rw , rs , and rf by taking arbitrary assigned optimization at each node (Section III-B). We further introduce the BoolGebra flow, including the node feature embeddings and the GNN model for logic optimization prediction (Section III-C), to shrink the orchestrated optimization search space and locate the optimization samples efficiently.

A. Optimization Space and Motivation

Our analysis (Figure 2) aims to explore and comprehend the optimization opportunities and space associated with minimizing AIGs via Boolean manipulations. Specifically, we employ a random sampling approach to generate various manipulation

B. Design Augmentation and Sampling

Here, we introduce our implementation for generating such random sampling solution and evaluate its AIG reduction performance, which is illustrated in Algorithm 1.

First, the algorithm takes the design in AIG representation $G(V, E)$ and the random decision for each node in vector D , which is stored in the file in csv format as inputs, where D is the same size of V . The three optimizations are encoded in integer indices, i.e., 0 for rw , 1 for rs , and 2 for rf . For example, $D[v] = 0$ indicates that for node v , the optimization 0, i.e., rw , is assigned for optimization. Subsequently, following the topological order, the algorithm checks the transformability of each node with respect to the assigned optimization operation $D[v]$ (line 2). If the optimization is applicable to the node for logic optimization, it is executed, resulting in the subgraph (the cut for node v) being updated (lines 3, 7) and the node itself is excluded from subsequent iterations. Conversely, if the

optimization cannot be applied to the node, it is skipped (line 5) for further optimizations. Algorithm 1 is implemented in ABC [5].

```

Input :  $G(V, E) \leftarrow$  Boolean Networks/Circuits in AIG
Input : Per node manipulation decision  $D$ ,  $|D| = |V|$ 
//  $D$  saved as an Array  $D$ , e.g.,  $D[1] = 0/1/2$ 
// indicates the optimization for node 1 is
//  $0/1/2$ , i.e.,  $rw/rs/rf$ .
Output : Post-optimized AIG  $G(V, E)$ 
1 for  $v \in V$  in topological order do
2   if  $v$  is transformable w.r.t  $D[v]$  then
3      $G(V, E) \xleftarrow{D[v]} G(V, E)$  continue // check the
// transformability with the assigned
// optimization
4   else
5     continue
6   end
7   Update  $G(V, E) \leftarrow$  Dec_GraphUpdateNetwork, and
// exclude  $v$  and transformed nodes from  $V$ 
8 end

```

Algorithm 1: Boolean manipulation sampling on AIGs

C. GNN-based prediction model

With multiple optimizations orchestrated in the algorithm, the optimization space become even larger, resulting in difficulties in locating the optimal solution efficiently. For example, for the design voter, whose original size is 13758, when orchestrating three operations in the logic optimization, the search space explodes to 3^{13758} , which is hardly possible to do exact explorations. Thus, to shrink the search space and locate the optimization direction efficiently, a GNN-based prediction model is proposed with AIG structure and initial feature embeddings as inputs and predicts the optimization performance directly. Note that the GNN-based model has strong generalization capability, thus, the model can train on small datasets but apply to large datasets for efficient inference optimization results.

In this section, we first introduce the dataset preparation for the model including the initial feature embeddings with structural and functional information for the AIG nodes, and the data normalization. Then, we introduce the structure of GNN-based model for logic optimization predictions.

1) *Dataset Preparation:* Utilizing the principles of message propagation and neighborhood aggregation within GNNs, we generate node embeddings for AIGs that effectively combine both structural and functional information. The structural information, i.e., the edgelist for the AIG, is integrated by transmitting node embeddings along edges. Second, the Boolean functional information can be encoded in node features. The initial node features are in two categories: (1) static features, where the features are static w.r.t the AIG structure, and will not alter with different optimization assignments; (2) dynamic features, where the features change as different assignments are given, which introduce different optimization results.

Feature Embedding – First, we extract the static features as shown in Figure 3 for each node. For the PI nodes (node a, b, c in Figure 3(a)), which have no fanins, the type features are all set as -99 . For the nodes with fanins, we attach 4 sets of features with 2 bits for each set, including:

1)-(a) – *the characteristics of AIG edges.* In AIG, the nodes are all 2-input AND nodes with edges inverted or not. From the left input edge to the right input edge, if the input edge is inverted, it will be encoded as 1; otherwise, encoded as 0. **Example:** As shown in Figure 3(b), the node d , whose left fanin edge is inverted and the right edge is not, is embedded with the node feature of $[1, 0]$. Note that since AIG is an universal representation and edge weights represent complement or not, this embedding is capable to incorporate local Boolean function.

1)-(b) – *rw transformability and local optimization gain* (third and fourth columns in Figure 3(c)). If rw is applicable for optimization at the node, then the third bit is set as 1 and the fourth bit is set as its corresponding optimization gain, i.e., the number of AIG minimization with the optimization applied; otherwise, if rw is not applicable, the third bit is set as 0, and the fourth bit is set as -1 . **Example:** In the AIG in Figure 3(a), for node p , it can be optimized with rw and its gain is 1. Thus, the feature embedding for node p is $[1, 1]$. However, for node d , which cannot be optimized by rw , its embedding is set as $[0, -1]$ at third and fourth bits.;

1)-(c) – *rs transformability and local optimization gain* (fifth and sixth columns in Figure 3(c)). **Example:** In the AIG in Figure 3(a), the node g can be optimized with rs and its gain is 3. Thus, the fifth bit and sixth bit are set as 1 and 3, respectively. For other inapplicable nodes with rs such as node p, m , and n , the fifth bit is set as 0 and the sixth bit is set as -1 .;

1)-(d) – *rf transformability and local optimization gain* (seventh and eighth columns in Figure 3(c)). **Example:** In Figure 3(a), the node g can be optimized with rf and its gain is 1, thus, its seventh and eighth bit in the feature embedding are set as 1 and 1, respectively. While for the node such as m , which is not applicable with rf , the seventh and eighth bits are 0 and -1 .

As a result, for each AIG node, its static feature embedding is an 8 dimensional vector containing information from its fanins, its transformability w.r.t orchestrated optimizations, i.e., rw, rs , and rf . For example, in Figure 3, the node g is embedded with features $[0, 1, 0, -1, 1, 3, 1, 1]$ for static feature embeddings. Note that these features are independent from the optimization sampling, which means they are static features dependent on the design structure only.

Second, for the dynamic feature as shown in Figure 3(d), for each node, it is a 4-bit one-hot representation. The embedding for PIs is set as $[-99, -99, -99, -99]$ to indicate they are PIs with no fanins. Then, for logic nodes, the dynamic feature indicates which operation is practically applied to the node under the specific optimization sampling. The 4 bits indicate none of optimizations is applied, rw is applied, rs is applied, rf is applied, respectively. The practically applied operation is set as 1 in one-hot representation while others are set as 0. For example, in Sample 2 (Figure 3(e)), node p is optimized with rw and the dynamic embedding for node p is thus $[0, 1, 0, 0]$ and node g is not optimized and its dynamic embedding is $[1, 0, 0, 0]$.

Note that the dynamic features vary according to the assignments under the current sampling, i.e., it depends not only on

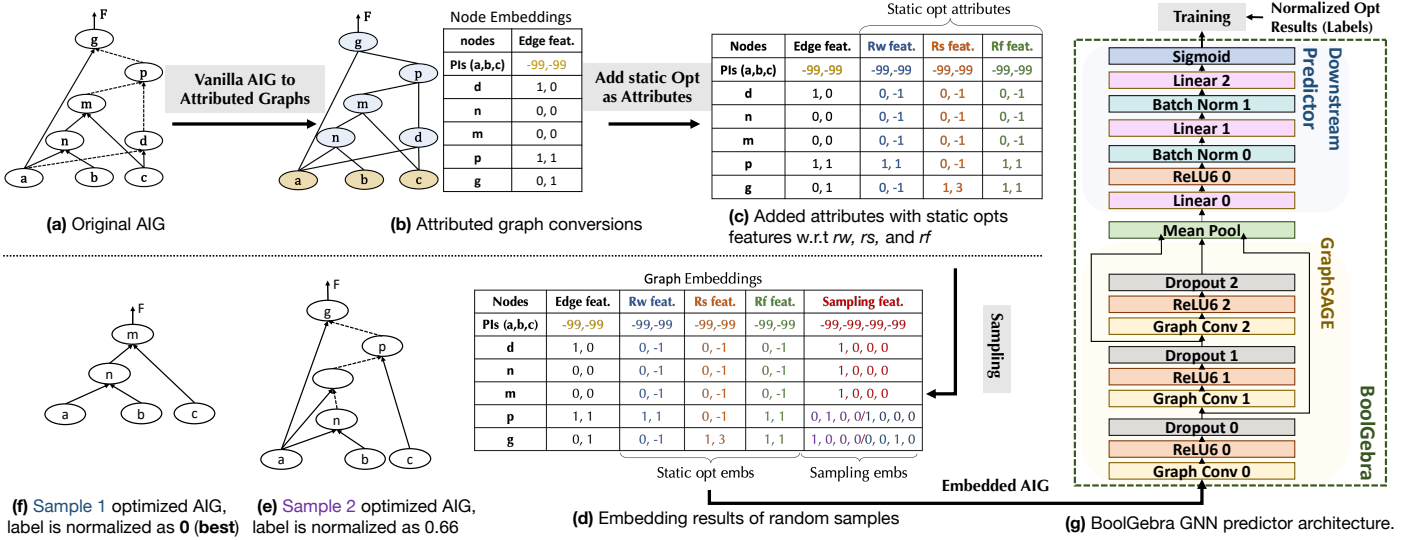


Fig. 3: The design flow of BoolGebra including the feature embeddings with static and dynamic sampling embeddings ((a) – (f)), and the model construction ((g)).

the design structure but also depends on the given optimization assignments. For example as shown in Figure 3, Figure 3(e) and Figure 3(f) are two different samples with two different dynamic assignments to node p and g , which lead to different samples with different feature embeddings and the corresponding optimization labels, which is referred as ground truth labels in the model training.

Data Normalization – The data distribution has significant importance on the model training and its performance. In this work, we find several challenges w.r.t the datasets during the training process: (1) the model overfits easily as the direct optimization results vary in a small range compared to its size number. For example, for the design `b12`, whose original AIG size is 1002, the best AIG optimization we observed is 952 and the worst is 1002. Thus the best AIG minimization is 50, which is only 5% of its size number 1002. That is, the labels for the samples are ranging from 95% to 100% w.r.t its original size; (2) the training data can be less distinctive within limited random samples as shown in Figure 2, i.e., purely random sampling can result in less various data samples, which can even worsen the overfitting problem in the model training.

Targeting the two challenges, we first normalize the AIG minimization w.r.t the highest node reduction number in the optimization samples, i.e., we set ratio of the gap between the node reduction in the current sample to the most node reduction of all the samples in the dataset as the label for the current sample. For example, for the two samples shown in Figure 3(e) and Figure 3(f), the best optimization for the dataset with these two samples reduces the AIG for 3 nodes as shown in Figure 3(f), thus, the label for Sample 1 (Figure 3(f)) is 0. While for Sample 2 in Figure 3(e), the reduction node number is 1 and its label is 0.66. Thus, we normalize the node reduction for the optimization samples into the percentage w.r.t the best AIG minimization ranging between $[0, 1]$. In this case, the model aims to relatively identify the best optimization candidates, rather than predicting the optimization results directly. By acquiring

the ratio number from the model, the selected most promising “optimal” samples with smaller ratio will be evaluated in ABC [5] for final evaluation.

To address the second challenge, we prioritize optimization techniques with minimal structural transformations during data sampling. Based on [6], we prioritize rw over rf to minimize structural changes. We assign different priorities to sampling options (rw , rs , and rf) and apply the highest priority operation to each node when applicable. Other applicable optimizations are randomly applied to nodes with lower priority. Using the initial sample, we generate additional data samples through partial random assignments, sampling a percentage of AIG nodes (10% to 90%) to create training data. The priority-guided random sampling produces more data samples with improved performance, enhancing the modeling training with efficient optimization structures as shown in Figure 2.

2) *GNNs Predictor*: As shown in Figure 3(g), the model takes the feature embedding at each node and the edgelist of the AIG as inputs and produces the AIG reduction as the prediction results. The model consists of two parts: the graph embedding part utilizing GraphSAGE [39] for attributed graph feature extraction and aggregation, and the prediction part employing multi-layer fully connected neural networks for predictions.

In the first part, the feature and structure embeddings of the AIG are fed into the model, and three GraphSAGE Convolution (Conv) layers are utilized. Each Conv layer is accompanied by a dropout layer with a dropout rate of 0.1 and a nonlinear layer (ReLU6). The hidden dimension of each Conv layer is 512, and the output dimension is 64. Following the feature embeddings obtained through GraphSAGE, the features are fused with a Pooling layer for concatenation with fully connected neural networks. The downstream model consists of three dense layers with output dimensions of 1000, 200, and 1 respectively, in order to complete the regression downstream model. The first linear layer is connected to an additional nonlinear layer (ReLU6), followed by a Batch Norm layer (BatchNorm 0). The results

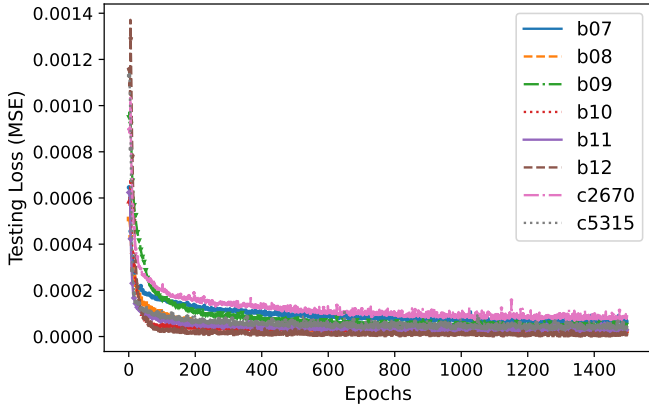


Fig. 4: Design-specific testing loss w.r.t training epochs.

from the Batch Norm layer are then connected to the second linear layer, which is combined with another Batch Norm layer (BatchNorm 1). Finally, the last linear layer is connected to a sigmoid layer to produce prediction results in the range of $[0, 1]$.

D. BoolGebra Flow

Finally, the aforementioned technical steps are integrated to form the BoolGebra flow. The BoolGebra flow comprises three key steps: (1) Random sampling of a large batch of Boolean manipulation decisions on a given AIG. (2) Pruning the randomly sampled design space using the GNN-based predictor. (3) Evaluation of the top solutions based on the prediction results obtained in step 2 to derive the final AIG reduction outcomes.

In this paper, we conduct our experimental results (Section IV) using a single BoolGebra flow, where the sampling, pruning, and evaluation steps are performed only once. Specifically, we employ a sampling size of 600 per design, and the top 10 results from the prediction phase are subsequently evaluated to determine their effectiveness.

IV. EXPERIMENTS

In this section, we present the experimental results of the proposed GNN-based AIG prediction model w.r.t its training performance on different designs, its design specific inference for each training design, and its cross design inference for different designs. Furthermore, we provide the comparison between the model selected optimization samples with the SOTA stand-alone optimizations to demonstrate the potential of the model in shrinking the search space and locating better optimization samples w.r.t various designs. All the experiments are conducted on Intel Xeon Gold 6230 20x CPU with RTX 3090 Ti GPU.

A. Design-Specific Evaluation

The proposed model in Section III-C is trained with the dataset with 600 priority guided random samples w.r.t each design. The training batch size is 100, using Adam [40] optimization algorithm with learning rate $8 \cdot 10^{-7}$. The decay rate

is 0.5 for every 100 epochs. Specifically, testing loss curves over 1500 training epochs with dataset of design b07, b08, b09, b10, b12, c2670, c5315 from ISCAS85 and ITC/ISCAS99 benchmarks, are shown in Figure 4. The model can coverage efficiently with all of the datasets, while the model trained with b12 and c5315 can result in better prediction performance with the smaller loss value.

Additionally, we visualize the prediction result versus the ground truth labels w.r.t each design in Figure 5, where the predicted values are the inference results of the training dataset with the same design specific trained model. For design b07 and design b10 as shown in Figure 5a and 5b, the ground truth labels are discrete due to its small node size (i.e., 366 and 180, respectively), and less graph structures for optimizations, resulting in worse model training performance. For design c2670 in Figure 5e, the prediction performs better at larger ground truth labels, while for better cases with smaller ground truth labels, the model can produce over-positive predicted results than actual labels as the training dataset contains much less data samples with better optimization, i.e., smaller ground truth labels (as shown in the sampling distribution in Figure 2) than the others, thus less accurate at the inference of better optimization samples. However, note that we do not expect to acquire exact optimization results from the model, we can still use the model to locate the most promising optimization samples. The model trained with design b11, b12 and c5315 show impressive correlation between the actual values and the predicted values.

B. Cross-Design Evaluation

Furthermore, we conduct the cross-design evaluations with combinations of different training designs and testing designs. The results are shown in Figure 6, including 9 combinations of training designs b11, c2670, and c5315, testing designs b11, b12, c2670, and c5315. The correlation trend in cross design inference is similar to the trend in design specific inference. Specifically, the model trained with design b11 shows better generalizability to other designs than other training designs. As shown in Figure 6a – 6c, the cross design evaluations show clean clustering trend similar to the design specific evaluations, which indicates the generalization capability of the proposed GNN-based prediction model.

C. Improvements over SOTA stand-alone optimizations

This section presents a comparative analysis between the exact node optimization results and the original And-Inverter Graph (AIG) node size. The top 10 optimized samples, as predicted by the model, were exclusively trained on a single design known as 'b11'. The corresponding outcomes are documented in Table 1. Specifically, we have included both the average performance (BG-Mean) of the predicted top 10 samples and the best result (BG-Best).

It should be noted that since the training was based on the 'b11' design, sample selections for other designs were inferred through cross-design considerations. When contrasted with state-of-the-art (SOTA) stand-alone optimizations like 'rw,' 'rs,' and 'rf,' the selected samples outperformed with a demonstrable

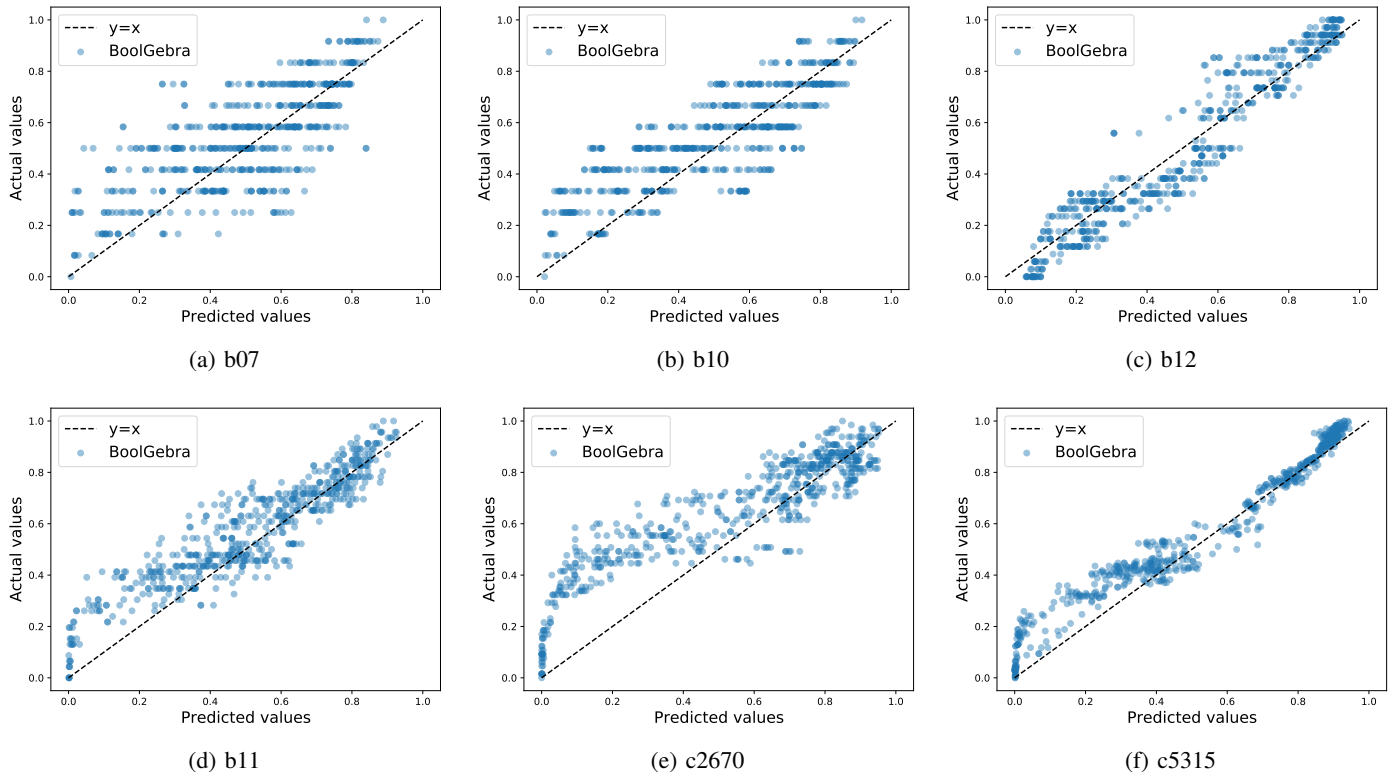


Fig. 5: Design-specific inference evaluation for predicting AIG minimization performance for given manipulation decisions. Each sub-figure corresponds to an individual design, where the inference input are unseen randomly sampled decisions, where x -axis represents the normalized prediction and y -axis represents the normalized ground truth. Note that value "0" refers to the best quality-of-results and "1" refers to the worst.

improvement in AIG optimization. Specifically, enhancements were measured at 3.6%, 5.3%, and 5.5% respectively, underscoring the potential of the BoolGebra flow. We want to point out that an average 3–5% logic minimization gain w.r.t SOTA logic synthesis is fundamentally significant.

TABLE I: Boolean minimization evaluations compared to state-of-the-art (SOTA) synthesis methodologies *rewrite*, *resub*, and *refactor* in ABC [5] framework. The results are presented in optimized AIG sizes (%) over the original AIG sizes. **Impr.(%)** refers improvements gained with BoolGebra-Best over the three SOTA methods. **BG** refers to BoolGebra.

Designs	<i>rewrite</i>	<i>resub</i>	<i>refactor</i>	BG (Mean)	BG (Best)
b07	0.981	0.975	0.959	0.940	0.934
b08	0.935	0.923	0.987	0.917	0.910
b09	0.978	0.971	0.993	0.956	0.956
b10	0.978	0.950	0.978	0.937	0.933
b11	0.895	0.897	0.881	0.834	0.828
b12	0.968	0.964	0.988	0.950	0.950
c2670	0.824	0.895	0.862	0.798	0.794
c5315	0.836	0.958	0.893	0.804	0.801
Avg	0.925	0.942	0.943	0.892	0.888
Impr.	3.6%	5.3%	5.5%	-	-

V. CONCLUSION

This work proposes a novel GNN-based AIG algorithmic space exploration flow BoolGebra to identify novel Boolean

manipulation decisions for the foundation of logic minimization. By introducing random sampling techniques, optimization and functional aware graph feature embedding, and the GNN model, BoolGebra can effectively identify top optimization candidates in the large random sample batch. Our model shows its potential in producing the promising optimization samples not only for design specific inferences but also for cross-design inferences. Our cross-design evaluation (trained with only one design) outperforms the three SOTA AIG optimization techniques with 3.6%, 5.3%, and 5.5% improvements. Our future work will focus on improving BoolGebra to identify novel Boolean manipulation solutions for technology-dependent stages such as mapping and placement.

Acknowledgement: This work is supported by National Science Foundation NSF-2047176, NSF-2019336, NSF-2008144, and NSF-2229562 awards.

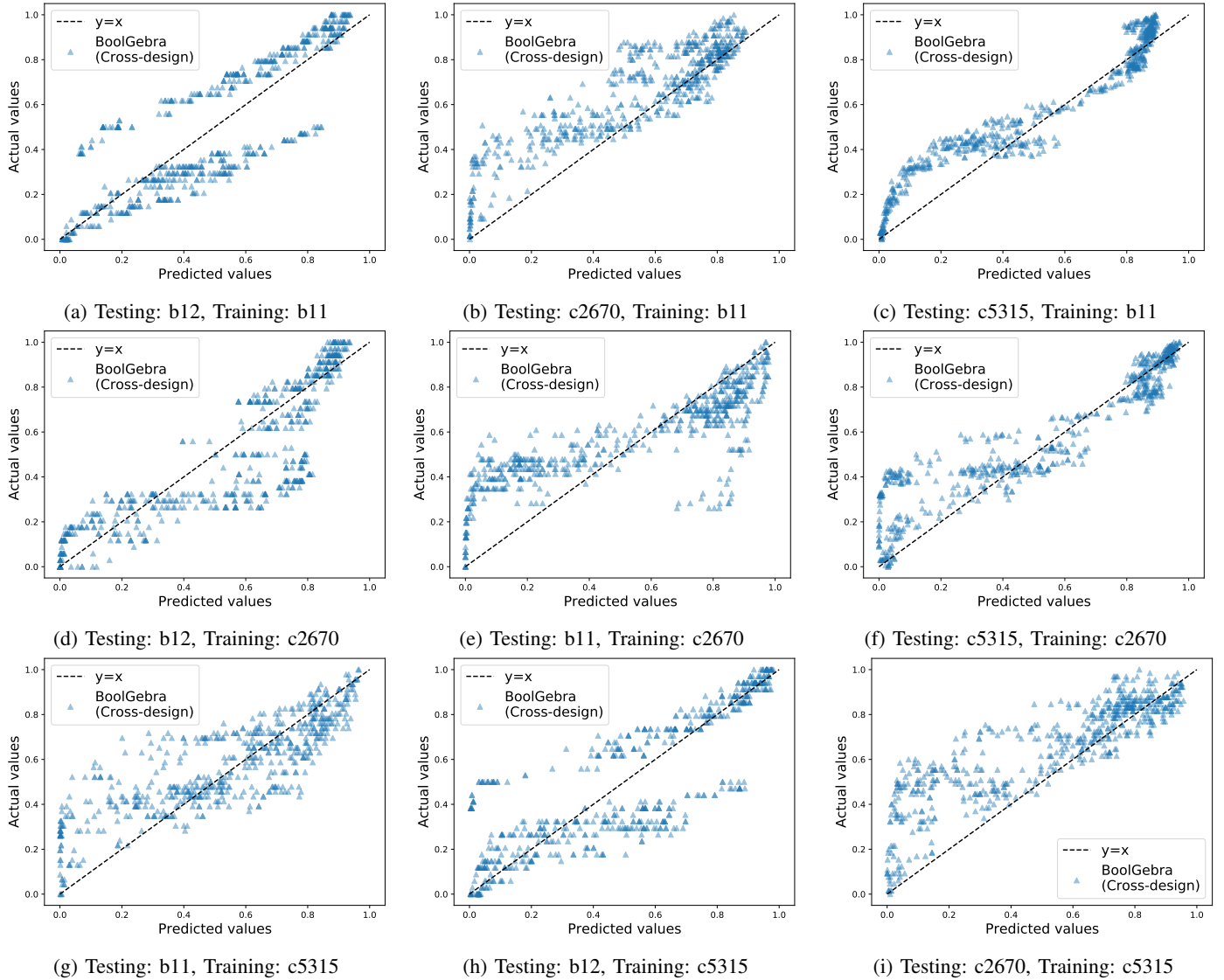


Fig. 6: Cross-design inference evaluation for predicting AIG minimization performance for given manipulation decisions. Each sub-figure presents the inference results versus the ground truth, where the model is trained on one design (Training) and tested on unseen design (Testing), denoted in the sub-captions.

REFERENCES

- [1] P. Bjesse and A. Borlvy, "Dag-aware circuit compression for formal verification," in *IEEE/ACM International Conference on Computer Aided Design, 2004. ICCAD-2004*. IEEE, 2004, pp. 42–49.
- [2] W. Haaswijk, E. Collins, B. Seguin, M. Soeken, F. Kaplan, S. Süssstrunk, and G. De Micheli, "Deep learning for logic optimization algorithms," in *2018 IEEE International Symposium on Circuits and Systems (ISCAS)*. IEEE, 2018, pp. 1–4.
- [3] R. K. Brayton, G. D. Hachtel, and A. L. Sangiovanni-Vincentelli, "Multilevel logic synthesis," *Proceedings of the IEEE*, vol. 78, no. 2, pp. 264–300, 1990.
- [4] L. Amaru, P.-E. Gaillardon, and G. De Micheli, "Majority-inverter graph: A new paradigm for logic optimization," *IEEE Transactions on CAD*, vol. 35, no. 5, pp. 806–819, 2015.
- [5] A. Mishchenko *et al.*, "Abc: A system for sequential synthesis and verification," URL <http://www.eecs.berkeley.edu/alanmi/abc>, vol. 17, 2007.
- [6] C. Yu, "Flowtune: Practical multi-armed bandits in boolean optimization," in *International Conference On Computer Aided Design (ICCAD)*. IEEE, 2020, pp. 1–9.
- [7] W. L. Neto, Y. Li, P.-E. Gaillardon, and C. Yu, "Flowtune: End-to-end automatic logic optimization exploration via domain-specific multi-armed bandit," *IEEE Transactions on Computer-Aided Design of Integrated Circuits and Systems*, 2022.
- [8] C. Yu, H. Xiao, and G. De Micheli, "Developing synthesis flows without human knowledge," in *Proceedings of the 55th Annual Design Automation Conference*, 2018, pp. 1–6.
- [9] A. Mishchenko, S. Chatterjee, and R. Brayton, "DAG-aware AIG Rewriting: A Fresh Look at Combinational Logic Synthesis," in *Design Automation Conference (DAC)*, 2006, pp. 532–535.
- [10] A. Mishchenko, S. Chatterjee, R. Jiang, and R. K. Brayton, "Fraigs: A unifying representation for logic synthesis and verification," ERL Technical Report, Tech. Rep., 2005.
- [11] C. Yu, M. Ciesielski, M. Choudhury, and A. Sullivan, "Dag-aware logic synthesis of datapaths," in *Proceedings of the 53rd Annual Design Automation Conference*, 2016, pp. 1–6.
- [12] C. Yu, M. Ciesielski, and A. Mishchenko, "Fast algebraic rewriting based on and-inverter graphs," *IEEE Transactions on Computer-Aided Design of Integrated Circuits and Systems*, vol. 37, no. 9, pp. 1907–1911, 2017.
- [13] M. Soeken, L. G. Amaru, P.-E. Gaillardon, and G. De Micheli, "Exact synthesis of majority-inverter graphs and its applications," *IEEE Transactions on CAD (TCAD)*, 2017.

- [14] Ç. Çalık, M. Sönmez Turan, and R. Peralta, "The multiplicative complexity of 6-variable boolean functions," *Cryptography and Communications*, vol. 11, no. 1, pp. 93–107, 2019.
- [15] W. Haaswijk, M. Soeken, L. Amarú, P.-E. Gaillardon, and G. De Micheli, "A novel basis for logic rewriting," in *ASP-DAC*. Ieee, 2017, pp. 151–156.
- [16] H. Riener, S.-Y. Lee, A. Mishchenko, and G. De Micheli, "Boolean Rewriting Strikes Back: Reconvergence-Driven Windowing Meets Resynthesis," in *ASP-DAC*, 2022.
- [17] W. Haaswijk, A. Mishchenko, M. Soeken, and G. De Micheli, "SAT based exact synthesis using DAG topology families," in *DAC*, 2018, pp. 1–6.
- [18] A. M. R. Brayton, "Scalable logic synthesis using a simple circuit structure," in *Proc. IWLS*, vol. 6, 2006, pp. 15–22.
- [19] L. Alrahis, A. Sengupta, J. Knechtel, S. Patnaik, H. Saleh, B. Mohammad, M. Al-Qutayri, and O. Sinanoglu, "Gnn-re: Graph neural networks for reverse engineering of gate-level netlists," *IEEE Transactions on Computer-Aided Design of Integrated Circuits and Systems*, vol. 41, no. 8, pp. 2435–2448, 2021.
- [20] G. Zhao and K. Shamsi, "Graph neural network based netlist operator detection under circuit rewriting," in *Proc. GLSVLSI*, 2022.
- [21] Z. He *et al.*, "Graph learning-based arithmetic block identification," in *Proc. ICCAD*, 2021.
- [22] N. Wu and Y. Xie, "A survey of machine learning for computer architecture and systems," *ACM Comput. Surveys*, 2022.
- [23] N. Wu, Y. Li, C. Hao, S. Dai, C. Yu, and Y. Xie, "Gamora: Graph learning based symbolic reasoning for large-scale boolean networks," *DAC*, 2023.
- [24] C. Yu and W. Zhou, "Decision making in synthesis cross technologies using lstms and transfer learning," in *Proceedings of the 2020 ACM/IEEE Workshop on Machine Learning for CAD*, 2020, pp. 55–60.
- [25] J. Yin, Y. Li, D. Robinson, and C. Yu, "Respect: Reinforcement learning based edge scheduling on pipelined coral edge tpus," *DAC*, 2023.
- [26] C. Yu and Z. Zhang, "Painting on placement: Forecasting routing congestion using conditional generative adversarial nets," in *Proceedings of the 56th Annual Design Automation Conference 2019*, 2019, pp. 1–6.
- [27] A. Hosny, S. Hashemi, M. Shalan, and S. Reda, "Drills: Deep reinforcement learning for logic synthesis," in *2020 25th Asia and South Pacific Design Automation Conference (ASP-DAC)*. IEEE, 2020, pp. 581–586.
- [28] Y. Li, M. Liu, M. Ren, A. Mishchenko, and C. Yu, "Dag-aware synthesis orchestration," *arXiv preprint arXiv:2310.07846*, 2023.
- [29] Z. Wang, C. Bai, Z. He, G. Zhang, Q. Xu, T.-Y. Ho, B. Yu, and Y. Huang, "Functionality matters in netlist representation learning," in *Proceedings of the 59th ACM/IEEE Design Automation Conference*, 2022, pp. 61–66.
- [30] E. Ustun, C. Deng, D. Pal, Z. Li, and Z. Zhang, "Accurate operation delay prediction for fpga hls using graph neural networks," in *Proceedings of the 39th International Conference on Computer-Aided Design*, 2020, pp. 1–9.
- [31] N. Wu, Y. Xie, and C. Hao, "Ironman: Gnn-assisted design space exploration in high-level synthesis via reinforcement learning," in *Proceedings of the 2021 on Great Lakes Symposium on VLSI*, 2021, pp. 39–44.
- [32] Y.-C. Lu, T. Yang, S. K. Lim, and H. Ren, "Placement optimization via ppa-directed graph clustering," in *Proceedings of the 2022 ACM/IEEE Workshop on Machine Learning for CAD*, 2022, pp. 1–6.
- [33] E. Ustun, S. Xiang, J. Gui, C. Yu, and Z. Zhang, "Lamda: Learning-assisted multi-stage autotuning for fpga design closure," in *2019 IEEE 27th Annual International Symposium on Field-Programmable Custom Computing Machines (FCCM)*. IEEE, 2019, pp. 74–77.
- [34] D. Pal, C. Deng, E. Ustun, C. Yu, and Z. Zhang, "Machine learning for agile fpga design," *Machine Learning Applications in Electronic Design Automation*, pp. 471–504, 2022.
- [35] L. Alrahis, J. Knechtel, and O. Sinanoglu, "Graph neural networks: A powerful and versatile tool for advancing design, reliability, and security of ics," in *Proceedings of the 28th Asia and South Pacific Design Automation Conference*, 2023, pp. 83–90.
- [36] S.-Y. Yu, R. Yasaei, Q. Zhou, T. Nguyen, and M. A. Al Faruque, "Hw2vec: A graph learning tool for automating hardware security," in *2021 IEEE International Symposium on Hardware Oriented Security and Trust (HOST)*. IEEE, 2021, pp. 13–23.
- [37] W. L. Neto, M. T. Moreira, L. Amaru, C. Yu, and P.-E. Gaillardon, "Read your circuit: leveraging word embedding to guide logic optimization," in *Proceedings of the 26th Asia and South Pacific Design Automation Conference*, 2021, pp. 530–535.
- [38] W. L. Neto, M. T. Moreira, Y. Li, L. Amaru, C. Yu, and P.-E. Gaillardon, "Slap: A supervised learning approach for priority cuts technology mapping," in *2021 58th ACM/IEEE Design Automation Conference (DAC)*. IEEE, 2021, pp. 859–864.
- [39] W. Hamilton, Z. Ying, and J. Leskovec, "Inductive representation learning on large graphs," *Advances in neural information processing systems*, vol. 30, 2017.
- [40] D. P. Kingma and J. Ba, "Adam: A method for stochastic optimization," *arXiv preprint arXiv:1412.6980*, 2014.